Received: 12 December 2018 | Revised: 19 March 2019 | Accepted: 22 March 2019

DOI: 10.1002/fam.2716

RESEARCH ARTICLE

WILEY

# Understanding structure ignition vulnerabilities using mock-up sections of attached wood fencing assemblies

**Sayaka Suzuki**[1] | **Samuel L. Manzello**[2]

[1] Large Fire Laboratory, National Research Institute of Fire and Disaster (NRIFD), Chofu, Japan

[2] Fire Research Division, National Institute of Standards and Technology (NIST), Gaithersburg, Maryland, USA

**Correspondence**
Sayaka Suzuki, Large Fire Laboratory, National Research Institute of Fire and Disaster (NRIFD), Chofu, Tokyo, Japan.
Email: sayakas@fri.go.jp

## Summary

Firebrand production from structure combustion becomes a key factor in the magnitude of how quickly a large outdoor fire may spread. Post-fire disaster investigations suggest that attached building components, such as wood fencing assemblies are known to be prone to ignition in these fires, and may provide pathways to structure ignition. Here, a comparison of ignition results from full-scale fencing assembly experiments conducted using a full-scale wind tunnel facility, to mock-ups of full-scale fencing assemblies using the recently developed experimental capability at the National Research Institute of Fire and Disaster (NRIFD) are discussed. In both experimental facilities, the fencing assemblies were exposed to firebrand showers using custom built continuous feed firebrand generators with size and mass distributions similar to those generated from structure combustion. Similar ignition behaviors were observed between the full-scale fencing assemblies and the mock-up of full-scale fencing assemblies. Additional experiments are required for other fencing assembly types to further verify these important findings.

**KEYWORDS**

large outdoor fire, ignition, firebrand

## 1 | INTRODUCTION

Large outdoor fires have the potential to create widespread destruction to the built environment. Recently, there have been significant number of wildfires that spread into communities and produced large-scale destruction over multiple continents across the globe. These fires are referred to as wildland-urban interface (WUI) fires. Another prominent example are large urban fires including those that have occurred after earthquakes. An important mechanism of structure ignition in both WUI and urban fires is the production of firebrands.

Post-fire studies have reported that attached building components may provide a pathway for structure ignition in these fires.[1-3] Examples of attached building components include wood fencing assemblies. The authors demonstrated that full-scale fencing assemblies may be ignited by firebrand showers, but the capability of the ignited fencing to transfer the fire to an adjacent structure, such as wall assembly, was not considered.[4]

As a result, this paper describes efforts to investigate the ability of firebrand showers to ignite wood fencing assemblies, and then observe the subsequent flame propagation along the ignited assembly to an *adjacent wall*. As this is a very complex problem, mock-up sections of full-scale fencing/wall assemblies were experimented with using unique experimental capabilities developed by the authors at the National Research Institute of Fire and Disaster (NRIFD). To be sure that mock-up sections may be used to provide useful insights, an extensive comparison of ignition results from full-scale fencing assembly experiments conducted using a full-scale wind tunnel facility, to mock-ups of full-scale fencing assemblies using the NRIFD facility was undertaken. In both experimental facilities, the fencing assemblies were exposed to firebrand showers using custom built continuous feed firebrand generators with size and mass distributions similar to those produced from burning structures.

Clearly, it is of interest to determine if similar fencing assembly ignition vulnerabilities were observed for reduced sized experiments.

  

Such information is required to guide the necessary configurations of fencing assembly mock-ups that can potentially be used in standard laboratory test methods. Furthermore, obtaining insights into ignition behavior from reduced sized experiments is a desirable tool.

Recent work, presented at a conference, reported that the evolution of the ignition process was similar for mock-up redwood lattice assemblies to the full-scale fencing assembly experiments.[5] In that study, the fencing assemblies *were not attached* to an adjacent wall. The present paper expands on these initial findings for presentation in the peer-reviewed literature.

## 2 | EXPERIMENTAL DESCRIPTION

### 2.1 | Full-scale experimental facility

The interested reader is referred elsewhere for a comprehensive description of the redesigned full-scale continuous feed firebrand generator system used here.[6] Namely, the feeding system was redesigned to be able to generate firebrand size and mass distributions using larger wood chips in an effort to produce a wider range of exposure conditions, as compared with prior studies.[6] Recent experiments have evaluated the performance of full-scale roofing components exposed to structure firebrand showers using this redesigned firebrand generator.[7] For completeness, a terse overview of the apparatus is provided presently.

The device consists of the main body and continuous feeding component. The main body of the generator was the same as prior investigations (Dragon component); the feeding system was rebuilt. The feeding system was connected to the main body and was equipped with two gates to prevent fire spread. In this experimental apparatus, airflow required for firebrand combustion/lofting was provided by a variable frequency drive blower that was coupled to the main body.[6] The airflow speed was initially varied to determine optimal operating conditions for glowing firebrand generation. In this work, the airflow used for firebrand generation had an average velocity of 2.0 m/s. These velocities were measured at the exit of the Dragon component using an anemometer. Due to the larger projected area of the wood chips used here, as described below, these blower speeds were lower than prior studies. A difficulty when constructing this device was designing a completely contained feeding system shielded from the wind tunnel flow.

The feeding system consisted of a pneumatic cylinder coupled to a cylindrical container where wood chips were stored (see Figure 1). Below the wood chip storage area, a plate was installed that allowed variation in the volume of wood chips to fall from the storage area to the first gate. This plate was set precisely to allow a specific mass of wood chips to fall into this volume. When the air pressure was applied, the sliding rod of the pneumatic cylinder moved forward and separated the wood chips from the storage area to the first gate, where they were then dropped into the second gate that leads to the Dragon where they are ignited (see Figure 1). The gate system was required to contain the fire from spreading from the Dragon to the feed system, and each gate was driven by pneumatic cylinders as well.

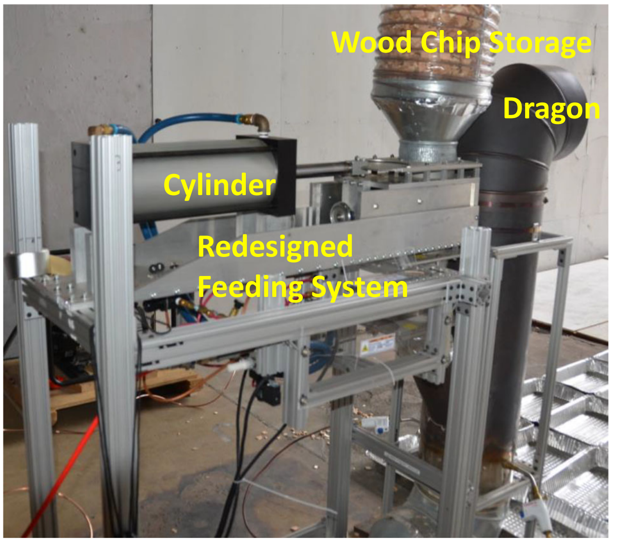


**FIGURE 1** Picture of full-scale continuous feed firebrand generator installed at the Building Research Institute's (BRI's) Fire Research Wind Tunnel Facility (FRWTF). Japanese cypress wood chips are feed into the device to produce firebrand showers similar to burning structures [Colour figure can be viewed at wileyonlinelibrary.com]

For all experiments, Japanese cypress wood chips were used to produce firebrands. These were provided from a supplier, and upon arrival, these chips were filtered using a 10-mm mesh to remove very fine wood pieces. The chips were also oven dried, as they were shipped under wet conditions. The sizes of wood pieces were selected to produce firebrands with larger projected area at a specific mass than our prior studies using continuous firebrand generation.[6] As structure firebrand production is an important factor in WUI and urban fire spread, the authors have begun to develop a database of firebrand production from burning structures/structure components and have demonstrated the ability to generate firebrands similar to structure firebrands from this database.[6] The sizes of Japanese cypress wood chips used for firebrand generation (before combustion) were 28 ± 8 mm (length), 18 ± 6 mm (width), and 3 ± 1.0 mm (thickness) (average ± standard deviation), respectively. The fencing assemblies, described below, were exposed to these structure firebrand showers.

As in prior experiments using the National Institute of Standards and Technology (NIST) Dragon, the new experimental device was installed inside the test section of Building Research Institute's (BRI's) Fire Research Wind Tunnel Facility (FRWTF). The facility was equipped with a 4-m-diameter fan to produce the wind field. The cross section of the FRWTF is 5 m wide by 4 m high. The maximum wind speed available using the FRWTF is 10 m/s. The leading edge fencing assemblies were placed at a distance of 3.25-m downstream of the full-scale continuous feed firebrand generator.

Redwood lattice fencing assemblies were constructed for the experiments (see Figure 2A,B). As shown in Figure 2A, these were custom fabricated by using two 1.22 m in height, 2.44 m in width,

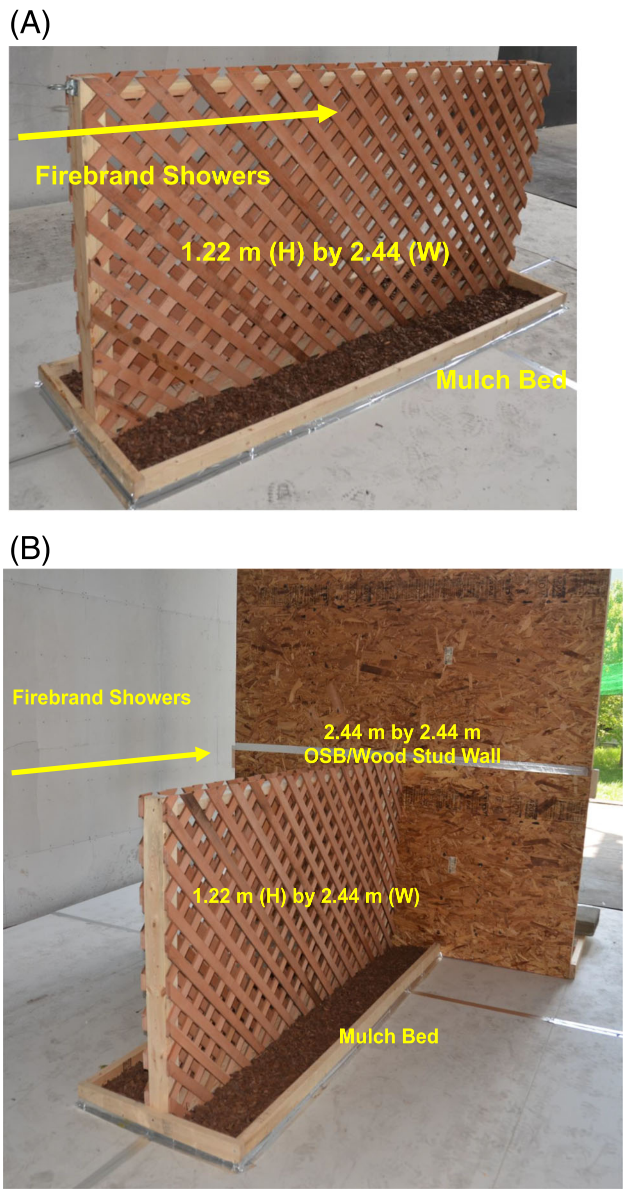


**FIGURE 2** A, Picture of full-scale redwood lattice fencing assembly with mulch bed. The dimensions were 1.22 m (H) and 2.44 m (W). B, Picture of full-scale redwood lattice fencing assembly attached to wall assembly with mulch bed. The attached wall assembly dimensions were 2.44 m (H) and 2.44 m (W) [Colour figure can be viewed at wileyonlinelibrary.com]

redwood lattice pieces and held together using a 2 × 4 wood array (2 × 4 boards are 38 mm by 89 mm). While two-sided redwood lattice fencing assemblies were used in this study, this type of fencing assembly may also be used in a one-sided configuration. The redwood lattice fencing assemblies were also attached to a 2.44-m by 2.4-m wall to simulate attachment to an adjacent structure (Figure 2B). Experiments are also underway to investigate these differences between one-sided and two-sided configurations, both at NIST and BRI/NRIFD. To simulate fine fuels that may be located near fencing assemblies, mini-pine bark mulch was used. Mini-pine bark nugget mulch was placed around the fencing assemblies at a depth of 51 mm (both sides). The mini-pine bark nuggets were oven dried, and the density was 0.15 g/cm$^3$. Pine bark nugget mulch is known to be harder to ignite than other types of mulch, so this mulch type was selected to be able to clearly see the dynamic ignition process. These redwood lattice fencing assembly/mulch beds were exposed to firebrand showers. Further details are shown in Figure 2A.

It was found that 170 ± 30 g, fed into the Dragon every 15 seconds, provided an adequate firebrand generation rate to ignite fencing assemblies. A supply of 170 g corresponded to approximately 560 wood pieces deposited every 15 seconds. The number flux (number of firebrands generated/m$^2$s), at the exit of the device, was measured at a feeding rate of 170 g every 15 seconds (680 g/min). To determine the number flux, the number of firebrands was counted at every frame of the video recording and summed every second. Based on the analysis, the number flux reached a steady value of 530/m$^2$s, 150 seconds after feeding began. Mass flux data (mass of firebrands generated/m$^2$s) were calculated by multiplying the number flux and the average mass of each firebrand at a feed rate of 170 g every 15 seconds.

The projected area of the firebrands directed at the fencing assembly/mulch bed was also quantified using a series of separate experiments where a water pan array was placed downstream of the firebrand generator. The firebrands were extracted and dried, and the mass, using a balance, and projected area, using image analysis methods, were determined. Figure 3 displays the projected area of the generated firebrands for various wind speeds (after combustion). In Figure 3, data are presented for *both* full-scale and reduced-scale

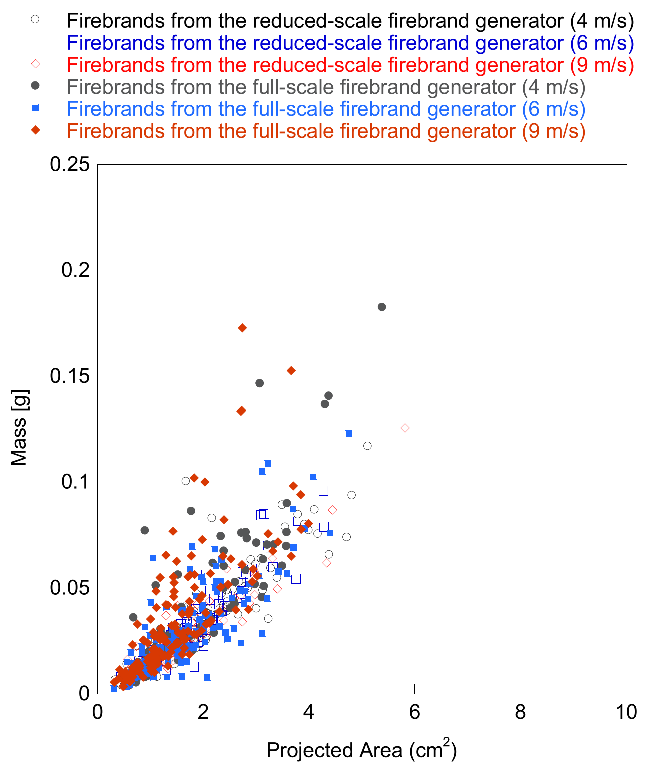


**FIGURE 3** Size and mass distribution of generated firebrands for full-scale and reduced-scale firebrand generators (after combustion) [Colour figure can be viewed at wileyonlinelibrary.com]

firebrand generators. The reduced-scale firebrand generator data, however, is described below. Image analysis software was used to determine the projected area of a firebrand by converting the pixel area using an appropriate scale factor. The standard uncertainty in determining the projected area was ±10%. The mass of each firebrand was measured by a precision balance. The standard uncertainty in the firebrand mass was approximately ±1%. The mean mass and standard deviation of each firebrand were obtained and observed to be 0.03 ± 0.02 g. Therefore, the mass flux of generated firebrands was calculated to be 16 g/m$^2$s for the full-scale firebrand generator.

## 2.2 | Experimental facility for mock-up assemblies

A reduced-scale continuous feed firebrand generator was used to generate firebrand showers. To couple it with wind facility at NRIFD, the original reduced-scale continuous feed firebrand generator was modified.[7] This reduced-scale continuous feed firebrand generator consisted of two parts: the main body and continuous feeding component. A comparison of the full-scale firebrand generator to the reduced-scale firebrand generator is shown in Figure 4. The feeding part was connected to the main body and had two gates to prevent fire spread. Each gate was opened and closed alternatively. A blower was also connected to the main body for the same reason as the full-scale firebrand generator. The blower speed at the Dragon's mouth was set to 4.0 m/s. When the blower was set to provide an average velocity below 4.0 m/s measured at the exit of the firebrand generator when no wood chips were loaded, insufficient air was supplied for combustion, and this resulted in a great deal of smoke being generated in addition to firebrands. Above 4.0 m/s, smoke production was mitigated but then many firebrands produced were in a state of flaming combustion as opposed to glowing combustion. In these experiments, glowing firebrands were desired to have a direct comparison with the full-scale experimental results. A longer main body was adapted so that only the firebrand generator part was above the stage, so the feeding part was not affected by wind. The efficacy of a smaller-sized firebrand generator to develop continuous firebrand showers has been described in detail elsewhere.[7]

A conveyor was used to feed wood pieces continuously into the device. For all tests, Japanese cypress wood chips were used to produce firebrands. These same size wood pieces were used in the full-scale fencing assembly studies (above) and have been shown to be within projected area/mass of burning structures. Specifics of the wood feeding rate are provided below. Recently, this facility has been used to expose mock-ups of full-scale roofing assemblies to firebrand showers, and the interested reader is referred elsewhere for a more comprehensive description of the NRIFD's facility.[7]

Since the base of the fan used to generate the wind field is located 1.6 m from the floor, the conveyor was placed under a custom stage designed for experiments when using the NRIFD wind facility (see Figure 5). The flow field was measured to be within ±10% over a cross section of 2.0 m by 2.0 m.

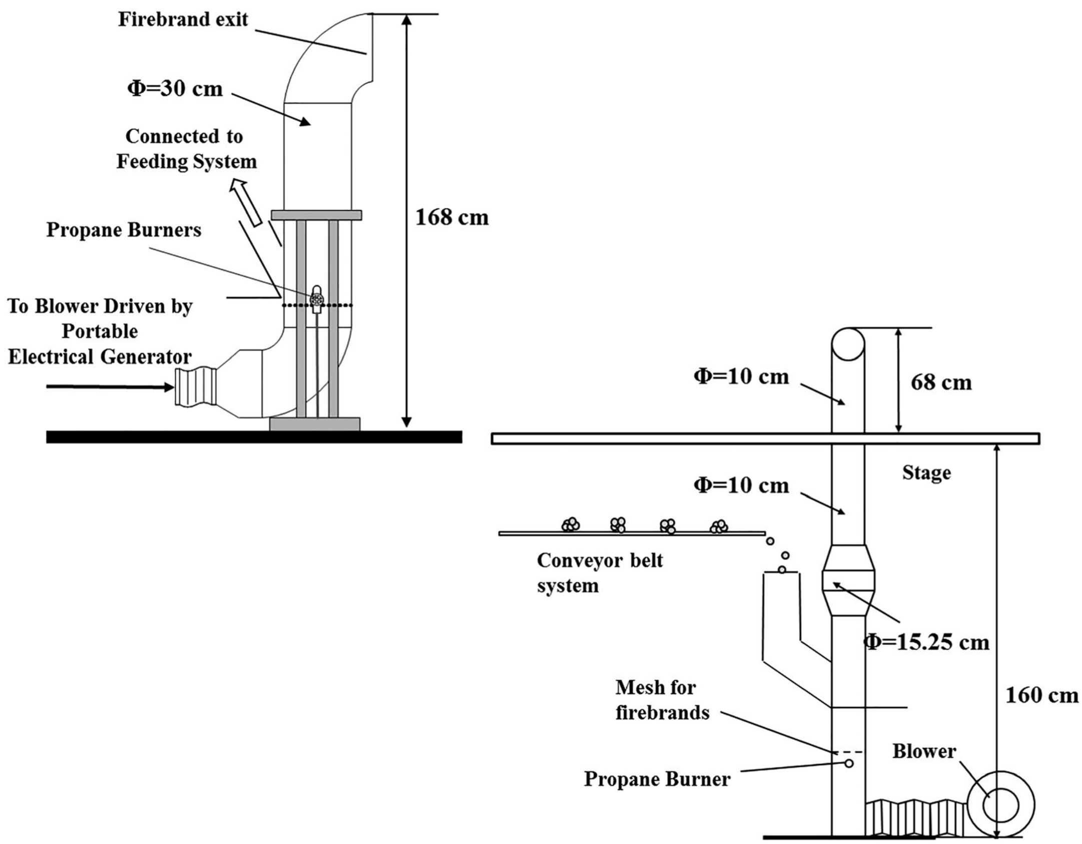


**FIGURE 4** A comparison of the full-scale (left-hand side) and reduced-scale firebrand generators[7]

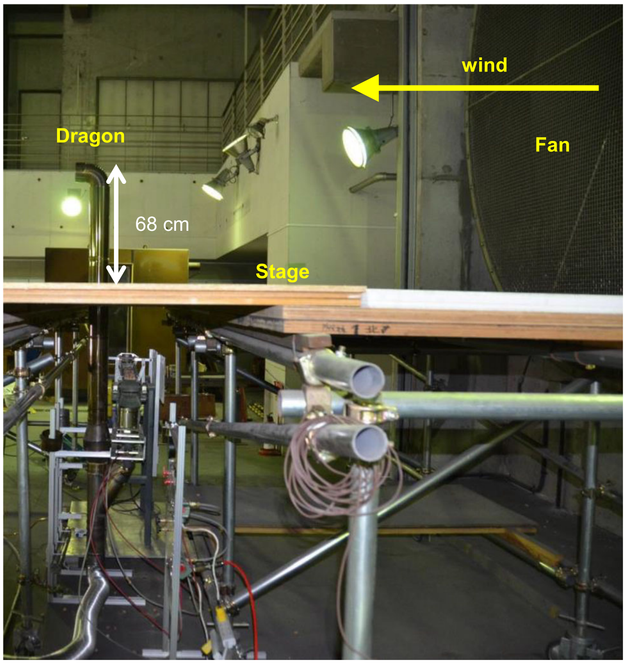


**FIGURE 5** Schematic of reduced-scale continuous feed firebrand generator installed at National Research Institute of Fire and Disaster's (NRIFD's) wind facility (side view). The diameter where the firebrands exit the firebrand generator (Dragon) was 10 cm. The stage dimensions were 5.5 m wide, 6.4 m long, with a height of 1.6 m [Colour figure can be viewed at wileyonlinelibrary.com]

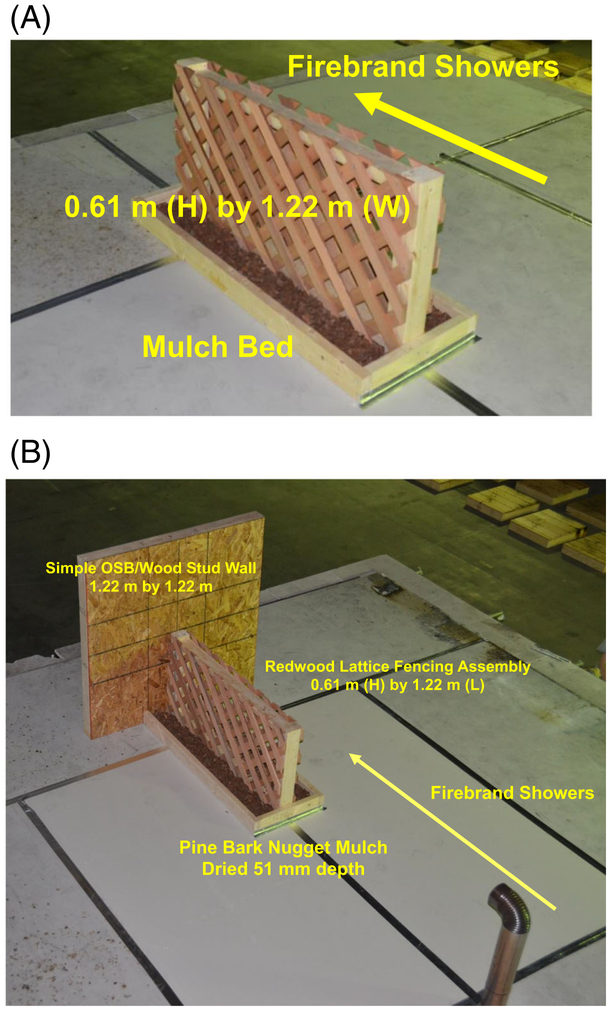


**FIGURE 6** A, Picture of mock-up of full-scale redwood lattice fencing assembly with mulch bed. The dimensions were 0.61 m (H) and 1.22 m (W). B, Picture of mock-up of full-scale redwood lattice fencing assembly with mulch bed. The wall assembly dimensions were 1.22 m (H) and 1.22 m (W). All mock-up assemblies were installed on top of the stage shown in Figure 5 [Colour figure can be viewed at wileyonlinelibrary.com]

Mock-ups of full-scale redwood lattice fencing assemblies were constructed for the experiments. The fencing assemblies were custom fabricated by using two 0.61 m in height, 1.22 m in width, redwood lattice pieces and held together using a 2 × 4 wood array (see Figure 6A). The redwood lattice fencing assemblies were also attached a 1.2 m by 1.2 m wall to simulate attachment to an adjacent structure (see Figure 6B). To simulate fine fuels that may be located near fencing assemblies, mini-pine bark mulch was used. Mini-pine bark nugget mulch was placed around the fencing assemblies at a depth of 51 mm (both sides). The mini-pine bark nuggets were oven dried and the density was 0.15 g/cm$^3$. The leading edge fencing assemblies were placed at a distance of 1.5-m downstream of the reduced-scale continuous feed firebrand generator in an effort to have the arrival number flux of firebrands similar to the full-scale experiments.

To expose the mock-ups of full-scale fencing assemblies to firebrand showers, a reduced-scale continuous feed firebrand generator was used. A conveyor was used to feed wood chips continuously into the reduced-scale firebrand generator. The conveyor belt was operated at 1.0 cm/s, and the wood chips were put on the conveyor belt at 12.5-cm intervals. The wood feed rate was fixed at 80 g/min, near the upper limit of reduced-scale firebrand generator. These same size wood chips were used in the full-scale roofing assembly study. Figure 3 displays the projected area of the generated firebrands at 6 and 9 m/s using the same analysis methods described for the full-scale continuous feed firebrand generator (see above).

## 3 | RESULTS AND DISCUSSION

### 3.1 | Full-scale fencing assemblies (no attached wall)

Experiments were conducted for wind speeds of 4, 6, and 9 m/s. In all cases, the evolution of the ignition process was similar. In total, three experiments were performed: one at each wind speed. Specifically, glowing firebrands ignited the mulch beds via smoldering combustion, and then the mulch transitioned to flaming combustion. These flaming mulch beds then ignited the redwood lattice fencing assemblies. Figure 7A displays the temporal evolution of the ignition process for a wind speed of 4 m/s. At the highest wind speed considered (9 m/s), once the fencing assembly was fully involved in flaming combustion, significant firebrand production from fence combustion was

(A)

(B)

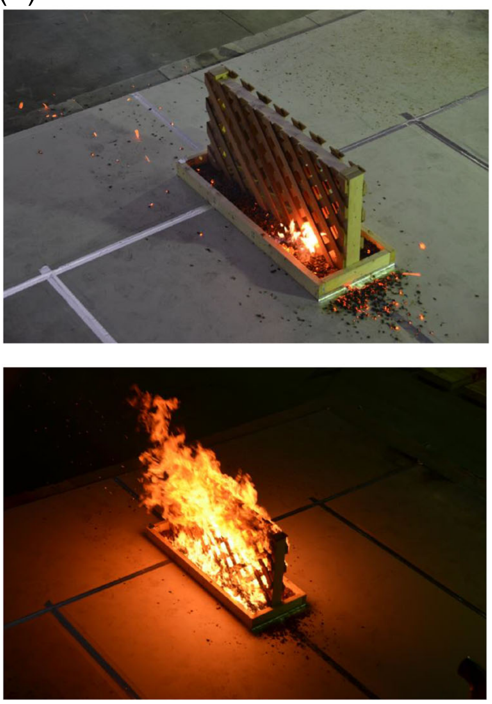

**FIGURE 7** A, Redwood lattice fencing assembly/mulch bed combustion with a wind speed of 4 m/s. The smoldering mulch bed has transitioned to flaming ignition, and the redwood lattice fencing assembly is ignited (top panel). In the bottom panel, the ignition has spread to the entire redwood lattice fencing assembly. B, Mock-up of full-scale redwood lattice fencing assembly/mulch bed combustion with a wind speed of 4 m/s. The dynamics of the ignition process is similar to full-scale experiment [Colour figure can be viewed at wileyonlinelibrary.com]

(A)

(B)

**FIGURE 8** A, Redwood lattice fencing assembly/mulch bed combustion with a wind speed of 9 m/s. Significant firebrand production may be observed. B, Mock-up of full-scale redwood lattice fencing assembly/mulch bed combustion with a wind speed of 9 m/s. Significant firebrand production may be observed [Colour figure can be viewed at wileyonlinelibrary.com]

observed (see Figure 8A; firebrands were observed to be transported outside the wind tunnel).

Not all the firebrands that are generated by the Dragon arrive at the fencing assembly/mulch bed. The average number of firebrands arriving on the mulch beds was counted as a function of wind speed. To simplify the analysis, firebrands were counted on the left-hand side of the mulch bed, and these values were doubled for the entire assembly. Based on these analysis, the average total arrival number flux of firebrands was 4/m$^2$s (average total arrival number flux based on results for 4- and 9-m/s wind speeds). As described below, efforts were made to try to have a similar firebrand arrival number flux for the mock-up experiments.

## 3.2 | Mock-ups of full-scale fencing assemblies (no attached wall)

Similar to the full-scale experiments, the wind speed was varied from 4 to 9 m/s. In all cases, the evolution of the ignition process was similar to the full-scale fencing assembly experiments. In total, three experiments were performed: one at each wind speed. Specifically, glowing firebrands ignited the mulch beds via smoldering combustion, and then the mulch transitioned to flaming combustion. These flaming mulch beds then ignited the redwood lattice fencing assemblies.

Figure 7B displays the temporal evolution of the ignition process for a wind speed of 4 m/s. At the highest wind speed considered (9 m/s), once the fencing assembly was fully involved in flaming combustion, significant firebrand production from fence combustion was also observed (see Figure 8B).

The average number of firebrands arriving on the mulch beds was counted as a function of wind speed. To simplify the analysis, firebrands were counted on the left-hand side of the mulch bed, and these values were doubled for the entire assembly. Based on these analysis, the average total arrival number flux of firebrands was 4.5/$m^2$s (average total arrival number flux based on results for 4 and 9 m/s wind speeds). It is important to note that similar ignition behaviors were observed between the full-scale fencing assemblies and the mock-up of full-scale fencing assemblies. Additional experiments are required for other fencing assembly types to further verify these important findings.

## 3.3 | Comparing ignition results—Attached Wall

Another series of experiments were conducted for wind speeds of 4, 6, and 9 m/s. In all cases, the evolution of the ignition process was similar. In total, seven experiments were performed: one at each wind speed for the mock-up assemblies and full-scale assemblies, respectively. At 6 m/s, another repeat experiment was performed for the full-scale assemblies. Specifically, glowing firebrands ignited the mulch beds (mini-pine bark mulch) via smoldering combustion, and then the mulch transitioned to flaming combustion. These flaming mulch beds then ignited the redwood lattice fencing assemblies. The ignited fencing assemblies then transferred the fire to adjacent walls. Figure 9A,B displays the ignition process for a wind speed of 6 m/s, for the full-scale and mock-up assemblies, respectively.

## 3.4 | Vertical flame height along the fencing assemblies

The maximum vertical flame heights, from the ground, at a given time were measured using detailed video records. As shown in Figures 7–9, due to air entrainment and the coupled wind effects, the flames were quite unstable. A three-point averaged flame height was adapted for this reason. The maximum vertical flame height at a given time was calculated as the average of flame heights over a 3-second interval. The average flame height was measured at every 30 seconds and at the time the flame reached the top of the fencing assembly. The average flame heights for all conditions are shown in Figure 10. Time 0 was the time the fencing assembly was ignited (blackened). The error bars represent the standard deviation. It was seen that flames were more unstable and propagated more quickly as they reached to the top of fencing assembly. The flame behavior was also affected by the ignition points (locations and the number of ignitions in the mulch beds), which is not controlled in this experimental series. For these

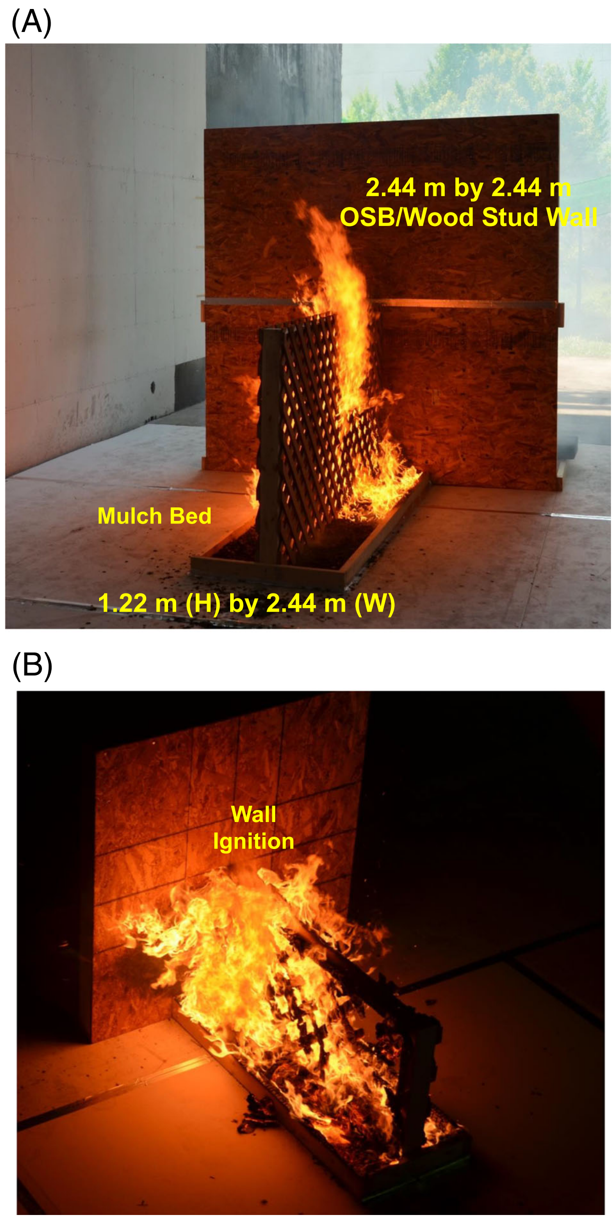


**FIGURE 9** A, Redwood lattice fencing assembly/mulch bed/wall assembly combustion with a wind speed of 6 m/s. Flame spread from the ignited fencing assembly to wall (6 m/s). B, Mock-up of full-scale redwood lattice fencing assembly/mulch bed/wall assembly combustion with a wind speed of 6 m/s. Flame spread from the ignited fencing assembly to wall (6 m/s). The dynamics of the ignition process is similar to full-scale experiment [Colour figure can be viewed at wileyonlinelibrary.com]

reasons, the maximum vertical flame travel rates, which are usually observed near the top of the fencing assemblies, was compared. The only exception was the full-scale experiment with no attached wall under a 9-m/s wind. In this case, the maximum vertical flame travel rate was observed in the middle of the assembly, rather than the end of the assembly. In this case, flame was constantly spread, shown in Figure 10.

Vertical flame travel rates were also determined based on measurements from the video records. Figure 11 shows the maximum

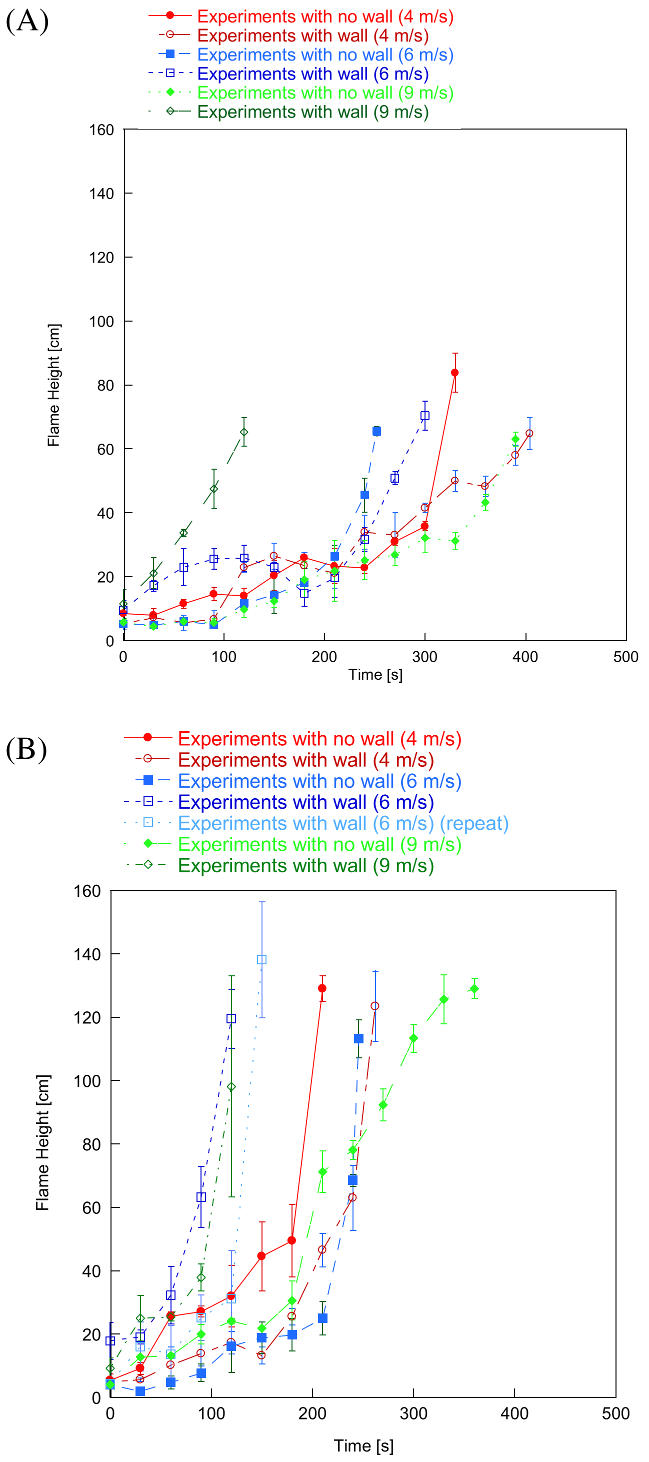


**FIGURE 10** Flame heights as a function of time for all experimental conditions. Time 0 is the time fencing assembly was ignited (blackened). A, Mock-up of full-scale redwood lattice fencing assembly. B, Full-scale redwood lattice fencing assembly [Colour figure can be viewed at wileyonlinelibrary.com]

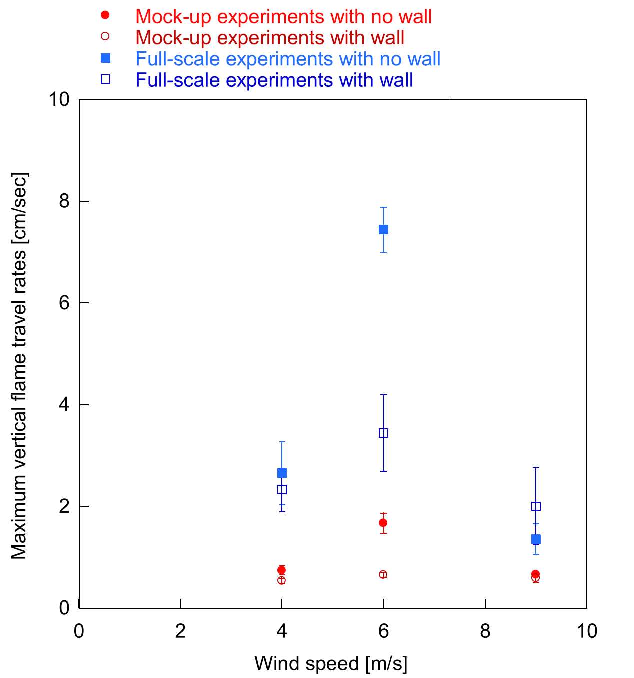


**FIGURE 11** Maximum vertical flame travel rates versus wind speed for all experimental conditions [Colour figure can be viewed at wileyonlinelibrary.com]

vertical flame travel rates under different wind speeds for the full-scale fencing assemblies and the mock-up fencing assemblies, with and without the attached wall. The maximum flame travel rate increased from 4 to 6 m/s and then decreased from 6 to 9 m/s for all cases. The existence of the wall reduced the maximum flame travel rate. The reduction for 6 m/s was observed to be the most for both full-scale and reduced-scale experiments, by 60% and 55%, respectively. The results that occurred at 6 m/s are quite interesting, but additional experiments are required to provide more quantitative explanations.

The interesting trends in flame dynamics are speculated to be the result of the porous nature of the lattice fencing assemblies and the more complex fluid dynamics as a result of the wall placement. Lattice fencing assemblies allow air to be easily entrained, as compared with solid or nonporous wood surfaces, resulting in extended flame heights protruding from the top of the assemblies. At higher wind speeds, there is also enhanced oxygen supply, yet when the wall is present, the stagnation zone in front of wall affects oxygen supply, and the enhanced recirculation leads to more unstable flames.

## 3.5 | Firebrands from fencing assemblies

The firebrands generated were collected from both the full-scale fencing assemblies and the mock-up fencing assembly experiments under a 9-m/s wind condition, respectively. Data are presented for these experiments without the presence of the wall, as there was no firebrand collection when wall assemblies were installed. Firebrands were collected after the experiments were completed and water pans were intentionally not used. The collection was carefully performed as not to confuse firebrands produced from the Dragon. These fencing assembly generated firebrands were compared with firebrands from the firebrand generators in Figure 12. Figure 12 shows that firebrands from redwood lattice fencing assemblies were almost 100 times bigger

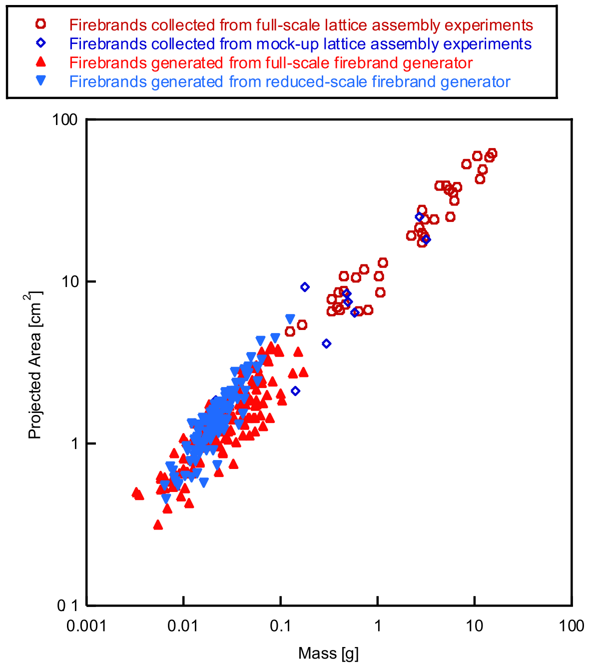


**FIGURE 12** Comparison of the size and mass of firebrands produced from firebrand generators and from fencing assemblies at both full-scale and mock-up experiments under a 9-m/s wind [Colour figure can be viewed at wileyonlinelibrary.com]

than those from the firebrand generators. It is interesting that despite the size differences, the relationship between mass and the projected area of firebrands from lattice fencing assemblies and the ones from firebrand generators is similar. Some of firebrands collected from fencing assemblies were able to keep some of construction features (Figure 13). These firebrands show some of breaking points for fencing assemblies for firebrand production. In this case, staples to keep fencing assemblies in place also can be still seen in firebrands. It is important to keep in mind that the collection methods were different, as water was not used to quench the firebrands produced from the fencing assemblies. Nonetheless, this comparison showed the possibilities

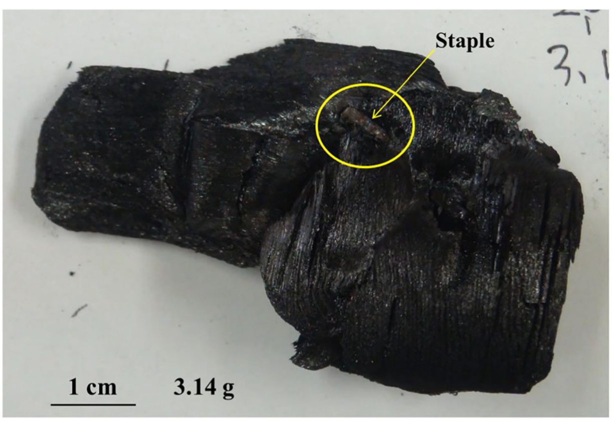


**FIGURE 13** The image of a firebrand produced from the fencing assembly under a 9-m/s wind at the bench-scale experiment. Staple was still observed [Colour figure can be viewed at wileyonlinelibrary.com]

of bigger firebrand production in WUI fires. Future experimental work should consider detailed studies to quantify firebrand production from fencing assemblies.

## 4 | SUMMARY

Fencing assemblies are known to be prone to ignition in WUI fires and may provide pathways to structure ignition. In this work, a comparison of ignition results from full-scale fencing assembly experiments conducted using a full scale wind tunnel facility to sections of full-scale fencing assemblies using the recently developed experimental capability at the NRIFD was presented. In both experimental facilities, the fencing assemblies were exposed to firebrand showers using custom built continuous feed firebrand generators with size and mass distributions similar to the structure firebrand database mentioned above.

Firebrand showers resulted in ignition of the full-scale redwood lattice fencing assemblies with mulch beds present. In all cases, the evolution of the ignition process was similar to the full-scale fencing assembly experiments. Specifically, glowing firebrands ignited the mulch beds via smoldering combustion and then the mulch transitioned to flaming combustion. These flaming mulch beds then ignited the redwood lattice fencing assemblies.

Naturally, further analyses of these interesting findings are in progress. Experiments are also required for other fencing assembly types to further verify these important findings. These results will provide guidance for further full-scale experimental campaigns focused on structure ignition by ignited fencing assemblies, such as those ongoing at the BRI (Japan), and those also currently in progress at NIST using burners for ignition, as compared with firebrand showers.[8]

Nevertheless, to be able to compare and contrast performance of various fencing types will require standardized testing methodologies. The results of the present study are providing the needed scientific understanding for important firebrand exposures.

## ACKNOWLEDGEMENT

Mr Marco Fernandez of NIST's Engineering Laboratory (EL) is acknowledged for shipping materials for the experiments.

## ORCID

*Sayaka Suzuki* https://orcid.org/0000-0002-6635-5512
*Samuel L. Manzello* https://orcid.org/0000-0002-3171-7333

## REFERENCES

1. Maranghides A, McNamara D, Vihnanek R, Restaino J, Leland C. A case study of a community affected by the Waldo Fire—event timeline and defensive actions. NIST TN1910. 2015.
2. Maranghides A, Mell W, Ridenour K, McNamara D. Initial reconnaissance of the 2011 wildland-urban interface fires in Amarillo, Texas. NIST TN1708. 2011.
3. Maranghides A, McNamara D. 2011 Wildland urban Interface Ammarillo Fires Report #2—assessment of fire behavior and WUI Measurement Science. NIST TN1909. 2016.

4. Suzuki S, Johnsson E, Maranghides A, Manzello SL. Ignition of wood fencing assemblies exposed to continuous-wind driven firebrand showers. *Fire Technol*. 2016;52(4):1051-1067.
5. Manzello SL, Suzuki S, Hagiwara I. Exposing fencing assemblies to firebrand showers characteristic of burning structures, fire and materials conference proceedings. 2017.
6. Manzello SL, Suzuki S. Generating firebrand showers characteristic of burning structures. *Proc Combust Inst*. 2017;36(2):3247-3252.
7. Suzuki S, Manzello SL. Experiments to provide the scientific-basis for laboratory standard test methods for firebrand exposure. *Fire Saf J*. 2017;91:784-790.
8. Johnsson E, Maranghides A. Effects of wind speed and angle on fire spread along privacy fences. NIST TN 1894. 2016.

**How to cite this article:** Suzuki S, Manzello SL. Understanding structure ignition vulnerabilities using mock-up sections of attached wood fencing assemblies. *Fire and Materials*. 2019;43:675–684. https://doi.org/10.1002/fam.2716